

8-2021

Characterizing the Role of UCHL5 in Metastatic Melanoma

Seenya Vincent

Follow this and additional works at: https://digitalcommons.library.tmc.edu/utgsbs_dissertations



Part of the [Medicine and Health Sciences Commons](#)

Recommended Citation

Vincent, Seenya, "Characterizing the Role of UCHL5 in Metastatic Melanoma" (2021). *The University of Texas MD Anderson Cancer Center UTHealth Graduate School of Biomedical Sciences Dissertations and Theses (Open Access)*. 1140.

https://digitalcommons.library.tmc.edu/utgsbs_dissertations/1140

This Thesis (MS) is brought to you for free and open access by the The University of Texas MD Anderson Cancer Center UTHealth Graduate School of Biomedical Sciences at DigitalCommons@TMC. It has been accepted for inclusion in The University of Texas MD Anderson Cancer Center UTHealth Graduate School of Biomedical Sciences Dissertations and Theses (Open Access) by an authorized administrator of DigitalCommons@TMC. For more information, please contact digitalcommons@library.tmc.edu.

Characterizing the Role of UCHL5 in Metastatic Melanoma

by

Seenya Vincent, BS

APPROVED:

Kunal Rai, Ph.D.

Advisory Professor

Menashe Bar-Eli, Ph.D.

Glen Traver Hart, Ph.D.

Min Gyu Lee, Ph.D.

Haoqiang Ying, M.D., Ph.D.

APPROVED:

Dean, The University of Texas

MD Anderson Cancer Center UTHealth Graduate School of Biomedical Sciences

Characterizing the Role of UCHL5 in Metastatic Melanoma

A

Thesis

Presented to the Faculty of

The University of Texas

MD Anderson Cancer Center UTHealth

Graduate School of Biomedical Sciences

in Partial Fulfillment

of the Requirements

for the Degree of

Master of Science

by

Seenya Vincent, BS

Houston, Texas

August 2021

Acknowledgements

Joining the Rai lab for the MS program has given me the opportunity to take part in exciting research, while surrounded by a wonderful team of colleagues. I'm also thankful to my advisory committee for guiding me on my projects, and the GSBS administrative office for always being available and supportive. I'm forever grateful to my parents, Vincent Mahapillai and Alice Vincent, for always believing in me and supporting me in everything that I do.

Characterizing the Role of UCHL5 in Metastatic Melanoma

Seenya Vincent, BS

Advisory Professor: Kunal Rai, PhD

Metastatic melanoma is one of the most aggressive cancers. In recent years, the survival rate has improved with the introduction of immunotherapy. Our lab conducted an *in vivo* ORF screen to identify potential drivers of metastasis. UCHL5/UCH37 was identified as one of the top candidates. UCHL5 is a deubiquitinating enzyme and interacts with the 26S proteasome complex and the INO80 chromatin remodeling complex. While UCHL5 has been shown to be overexpressed in many cancers, it has not been well characterized in melanoma. We investigated the role of UCHL5 in metastatic melanoma *in vitro* through overexpressing and knocking down UCHL5 in primary and metastatic melanoma cell lines, Western Blotting, RNA-sequencing, ATAC-sequencing, ChIP-sequencing, and *in vivo* by using a mouse model. Mice that were inoculated with B16F10 shUCHL5 cells and subsequently treated with an isotype control led to reduced tumor burden. However, mice that were inoculated with B16F10 shUCHL5 cells and were also treated with anti-mouse PD1 led to increased tumor burden. We find that UCHL5 plays a role in the progression of metastatic melanoma and contributes to an increased tumor burden. These findings can provide insight into how we approach treatment for metastatic melanoma, including how we target and modulate the function of UCHL5.

Table of Contents

<i>Approval Page</i>	<i>i</i>
<i>Title Page</i>	<i>ii</i>
<i>Acknowledgements</i>	<i>iii</i>
<i>Abstract</i>	<i>iv</i>
<i>Table of Contents</i>	<i>v</i>
<i>List of Illustrations</i>	<i>vii</i>
<i>List of Tables</i>	<i>viii</i>
<i>Chapter 1: Introduction</i>	<i>1</i>
<i>1.1 Background</i>	<i>1</i>
<i>1.1.1 Melanoma</i>	<i>1</i>
<i>1.1.2 Discovery, Identification, and Characterization of UCHL5</i>	<i>2</i>
<i>1.1.3 UCHL5 in Normal Physiology</i>	<i>3</i>
<i>1.1.4 UCHL5 in Disease</i>	<i>4</i>
<i>1.2 Rationale and Hypothesis</i>	<i>5</i>
<i>1.2.1 In vivo ORF screen for pro-metastatic epigenetic drivers of melanoma</i> ...	<i>5</i>
<i>1.2.2 Summary, Hypothesis, and Specific Aims</i>	<i>11</i>
<i>Chapter 2: Methods and Materials</i>	<i>12</i>
<i>2.1 Cell Lines</i>	<i>12</i>
<i>2.2 Plasmid Preparation</i>	<i>12</i>
<i>2.3 Lipid-Based Transfection and Lentivirus Generation</i>	<i>12</i>
<i>2.4 Generation of UCHL5 Knockdown and Overexpression Cell Lines</i>	<i>13</i>
<i>2.5 Western Blotting</i>	<i>13</i>
<i>2.6 RNA-Sequencing</i>	<i>14</i>
<i>2.7 ATAC-Sequencing</i>	<i>14</i>
<i>2.8 ChIP-Sequencing</i>	<i>15</i>
<i>2.9 Mice</i>	<i>15</i>
<i>2.10 Mouse Experiments</i>	<i>15</i>
<i>2.11 Flow Cytometry</i>	<i>16</i>
<i>2.12 Statistical Analysis</i>	<i>18</i>

Chapter 3: Results	19
3.1 UCHL5 knockdown in vitro alters chromatin accessibility and promotes enhancer/super-enhancer reprogramming in metastatic melanoma	19
3.2 UCHL5 knockdown combined with anti-PD1 treatment increases tumor burden in mice	25
3.3 UCHL5 knockdown combined with anti-PD1 treatment may alter the immune microenvironment.....	30
Chapter 4: Discussion, Future Directions, and Conclusions.....	33
4.1 Discussion.....	33
4.2 Future Directions	37
4.3 Conclusions	39
Bibliography.....	41
Vita	52

List of Illustrations

<i>Figure 1. An epigenetic ORF screen identified UCHL5 as a pro-metastatic driver of melanoma.....</i>	<i>6</i>
<i>Figure 2. UCHL5 promotes invasion</i>	<i>8</i>
<i>Figure 3. UCHL5 is overexpressed in metastatic melanoma</i>	<i>9</i>
<i>Figure 4. UCHL5 employs INO80 chromatin remodeling activity for promoting melanoma invasion.....</i>	<i>10</i>
<i>Figure 5. Confirmation of UCHL5 knockdown in WM266-4 by Western Blotting</i>	<i>21</i>
<i>Figure 6. ATAC-seq shows UCHL5 knockdown alters accessibility in regulatory regions</i>	<i>22</i>
<i>Figure 7. ChIP-seq reveals that UCHL5 knockdown promotes enhancer/super-enhancer reprogramming.....</i>	<i>23</i>
<i>Figure 8. UCHL5 knockdown alters mesenchymal gene expression</i>	<i>24</i>
<i>Figure 9. Validation of UCHL5 knockdown in B16F10 mouse melanoma cell lines.....</i>	<i>27</i>
<i>Figure 10. Schematic of mouse experiment</i>	<i>28</i>
<i>Figure 11. UCHL5 knockdown combined with anti-PD1 treatment increases tumor burden.....</i>	<i>29</i>
<i>Figure 12. Exhausted T cells may be altered upon UCHL5 knockdown and PD1 blockade</i>	<i>31</i>
<i>Figure 13. Memory T cells may be altered upon UCHL5 knockdown and PD1 blockade</i>	<i>32</i>
<i>Figure 14. UCHL5 interacts with YAP1.....</i>	<i>36</i>
<i>Figure 15. Overlap of UCHL5-occupied genes and differential gene expression shows ARHGAP29 as a UCHL5 target</i>	<i>38</i>
<i>Figure 16. Model of UCHL5 interactions, regulatory activity, and downstream targets.....</i>	<i>40</i>

List of Tables

<i>Table 1. Panels run for flow cytometry</i>	<i>17</i>
---	-----------

Chapter 1: Introduction

1.1 Background

1.1.1 Melanoma

Melanoma is considered to be an aggressive cancer. While it's not the most common skin cancer [1], it tends to be more aggressive than other skin cancers because of its ability to metastasize quickly [2]. Melanoma occurs when melanocytes, which are derived from neural crest cells, are malignantly transformed [2]. About half of all melanoma cases also have activating BRAF mutations [2]. The introduction of immune checkpoint blockade (ICB), which began with Ipilimumab in 2011 [3] and targets Cytotoxic T-lymphocyte-associated protein 4 (CTLA-4), and which was followed by Pembrolizumab and Nivolumab targeting Programmed Cell Death Protein-1 (PD-1), has improved the prognosis of patients with melanoma in terms of both survival and tumor recurrence rates [2, 3, 4, 5]. In recent years, the 5-year survival rate for early-stage melanoma has increased to 98.3% [3]. However, the outlook for metastatic melanoma is still dire with a 5-year survival rate of just 16% [3].

Patients with metastatic melanoma face several challenges with regard to effectiveness of treatment. One of these issues is acquired resistance to treatment, including immunotherapy, which can lead to recurrence of melanoma [2, 3]. One of the underlying causes of resistance to immunotherapy is secondary genomic aberrations [4]. Epigenetic therapy, either alone or in combination with immune checkpoint blockade, has been shown to improve the effectiveness of treatment against metastatic melanoma [4]. This has opened the door to investigating new targets within the genome and epigenome.

1.1.2 Discovery, Identification, and Characterization of UCHL5

In 1997, a yet-to-be named deubiquitinating enzyme (DUB) was discovered when PA700/19S regulatory particle, a subunit of the 26S proteasome, was purified from bovine red blood cells [6]. It was later named Ubiquitin C-terminal hydrolase 37 (UCH37) [7], and is also known as UCHL5, in mice [8]. Human UCH37 and mouse UCHL5 are nearly 100% identical [8,9], and the terms are used almost interchangeably in the scientific literature. UCH37 was elucidated by doing Ubiquitin isopeptidase activity assays and affinity labeling of the unknown DUB with Ub-nitrile [6]. Specifically, UCH37 was found to act on the Lys48-linked diubiquitin substrate [6]. The association of UCH37 with PA700 was determined by co-sedimentation with isopeptidase inhibitor Ub-aldehyde [6]. The molecular mass of UCH37 was determined to be 37 kDa [6,9]. An X-ray crystal structure of the full-length UCH37 was also generated [10]. Chromatographic analysis of UCH37 showed that low protein concentrations of UCH37 may show varied and inaccurate activity, and UCH37's average molecular weight actually increases as a function of its concentration [10]. Human *UCH37* is located on chromosome 1 and contains 12 exons [11].

There are around 100 putative deubiquitinating enzymes, which can be classified into 5 families, including the Ubiquitin C-terminal (UCH) family [12]. The 4 members of the UCH family are UCHL1, UCHL3, UCHL5/UCH37, and BAP1 [9,13]. UCH37 is well-conserved, including in humans, mice, fruit flies, and fission yeast [9].

UCH37 contains both an N-terminal catalytic domain, and a non-conserved extended C-terminal tail [8,10]. UCH37 interacts with 2 different complexes: the INO80 chromatin remodeling complex, and the 26S proteasome [9,14]. Nuclear factor related

to kappa-B-binding protein (NFRKB) recruits UCH37 to the INO80 complex which remodels chromatin by sliding nucleosomes [9,15,16]. INO80 is also recruited by the transcription factor, YY1 [15]. The 26S proteasome degrades polyubiquitinated proteins [9]. UCH37 cannot act alone, and instead has to be recruited by RPN13 (ortholog of ADRM1) to the 26S proteasome [7,10,17,18]. In fact, UCH37 has an autoinhibitory tail, with a KEKE motif, in the C-terminal domain that prevents it from deubiquitinating substrates on its own [7,13]. However, it is possible for UCH37 to self-assemble and form an oligomer at high concentrations [10]. UCH37 can interact with only 1 of the 2 complexes at any given time because NFRKB and RPN13 competitively bind to UCH37's C-terminal [7,9,16,19], even though they interact in a similar manner with UCH37 [9,18]. The activity of UCH37 is controlled by RPN13 and NFRKB [20]. UCH37 is activated when bound by RPN13 and recruited to the 26S proteasome [16,21]. UCH37 is inactive, both in the nucleus, as well as when bound by NFRKB in the INO80 complex [16]. In this state, UCH37 cannot perform deubiquitination. Oddly enough, human RPN13 can activate UCH37 while it is bound to INO80, but the resulting deubiquitinating activity is very low, and possibly ineffective [16]. UCH37 acts on Lys48-linked polyubiquitin substrates, where it removes ubiquitin from the distal end [7,8,10,21,22]. Ubiquitin-mediated proteolysis occurs when a protein is tagged with ubiquitin, which marks it for degradation by the 26S proteasome [23].

1.1.3 UCHL5 in Normal Physiology

UCH37 is essential in several areas. UCH37 is required for cell cycle progression [24]. It also plays a role in DNA repair through double-strand end break resection and homologous recombination [25].

UCH37 has been shown to function in TGF- β signaling by interacting with Smad transcription factors, including Smad 2, Smad 3, and especially Smad7 [8].

UCH37 also interacts with β -catenin, a signal transduction protein in the Wnt/ β -catenin pathway and prevents its degradation [11]. This involvement in both TGF-B signaling and the Wnt/B-catenin pathways could also contribute to cancer because these pathways are essential. UCHL5 is also necessary for brain development in mice, as well as their survival [26]. Complete deletion of *Uch37* results in prenatal lethality of mice [26].

1.1.4 UCHL5 in Disease

UCHL5 has been shown to be aberrantly expressed in disease states, including cancer and Alzheimer's disease. UCHL5 is overexpressed in multiple cancers, including HPV+ cervical carcinoma [27], hepatocellular carcinoma [28], epithelial ovarian cancer [13,29], multiple myeloma [12], Waldenstrom Macroglobulinemia [30], non-small cell lung cancer [14], esophageal squamous cell carcinoma [13,14], pancreatic cancer [13], as well as gastric and colon cancers [14]. *In vitro* assays of hepatocellular carcinoma cell (HCC) lines have shown that UCH37 could be promoting cell migration and invasion [28]. In epithelial ovarian cancer (EOC), UCHL5 expression was higher in less differentiated tumors, and was also linked to worse prognosis [29]. In HCC and EOC, UCHL5 prevents the degradation of proteins that should be degraded and can also be considered a prognostic factor for time to recurrence [28,29]. UCHL5 is, therefore, considered to be a tumor promoter [13]. Interestingly, UCHL5 is downregulated in Alzheimer's disease, and affects the relationship between proteolysis and transcriptional regulation [31].

1.2 Rationale and Hypothesis

1.2.1 *In vivo* ORF screen for pro-metastatic epigenetic drivers of melanoma

It is well known that the progression of many cancers, including melanoma, can be driven by genetic alterations [32, 33, 34]. However, there is still a gap of knowledge regarding epigenetic alterations that drive melanoma. Our lab conducted a gain-of-function (overexpression), gain-of-phenotype (metastasis) screen using 430 ORFs belonging to 358 epigenetic genes, to identify pro-metastatic epigenetic genes in melanoma (Fig 1A). These ORFs were overexpressed in a pooled fashion (15 genes per pool) in a genetically engineered partially transformed tumorigenic but non-metastatic primary melanocyte system (pMEL-BRAF-shPTEN) which generates non-metastatic tumors in 9-15 weeks upon xenotransplantation. All 310 mice (10 mice for 31 pools) were monitored for nodules in the lung, liver, and lymph nodes, and hits were identified from metastatic lesions through PCR and sequencing. UCHL5 was identified as a top candidate, amongst 9 other genes, in the screen (Fig 1B). Lungs from mice injected with UCHL5 expressing WM115 cells (primary melanoma) showed nodules, but not mice injected with GFP expressing WM115 cells (Fig 1C). A point mutant derivative was also generated for UCHL5 (C88S), which abrogated the catalytic activity of UCHL5. Mice that were injected with UCHL5 overexpressing pMEL-BRAF-shPTEN, WM115, or WM793B cells all had more metastases compared to mice that were injected with the same 3 cell lines expressing GFP or UCHL5 C88S (Fig 1D).

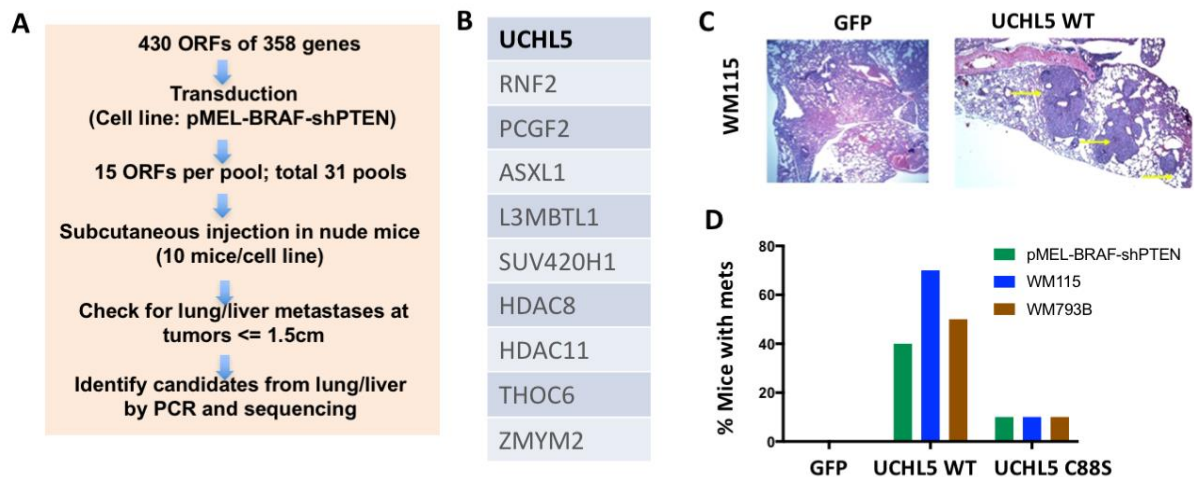


Fig 1. An epigenetic ORF screen identified UCHL5 as a pro-metastatic driver of melanoma. (A) Experimental design of an *in vivo* overexpression screen to identify pro-metastatic epigenetic genes regulating melanoma. (B) Gene-hits after secondary validation. (C) Images of lungs from mice injected with GFP or UCHL5 expressing WM115 cells. (D) Graph showing percent of mice with lung nodules after mice injected with GFP, wild type (WT) or Catalytic mutant (CM) UCHL5 expressing cells in pMEL-BRAF^{V600E}-shPTEN, WM115 or WM793B backgrounds.

We performed Boyden chamber assays to determine invasive potential and found that invasion is substantially decreased in cells expressing GFP or UCHL5 C88S, compared to cells expressing UCHL5 WT (Fig 2). This indicated that UCHL5 promotes invasion. We also surveyed existing mRNA expression databases for UCHL5 expression in matched primary and metastatic melanoma tissues and noted that Xu et al [35] showed increased expression of UCHL5 in metastatic tissues compared to primary tumors (Fig 3). UCHL5 has also previously been shown to interact with the INO80 chromatin remodeling complex [9]. We wanted to know whether INO80 is required for the invasive activity of UCHL5 expressing cells. We knocked down INO80 and assessed invasion activity. We found that UCHL5 employs INO80 for invasion in melanoma (Fig 4).

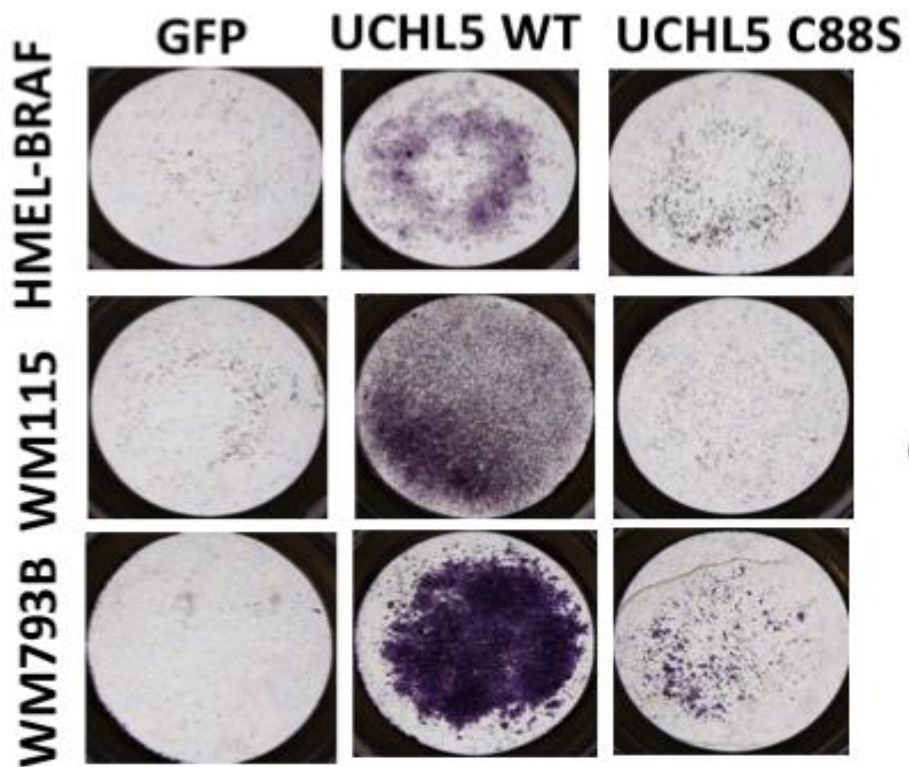


Fig 2. UCHL5 promotes invasion. Images of invasive cells after Boyden chamber assay on pMEL-BRAF^{V600E}-shPTEN, WM115 or WM793B cells overexpressing GFP, wild type (WT) or catalytic mutant (C88S) version of UCHL5.

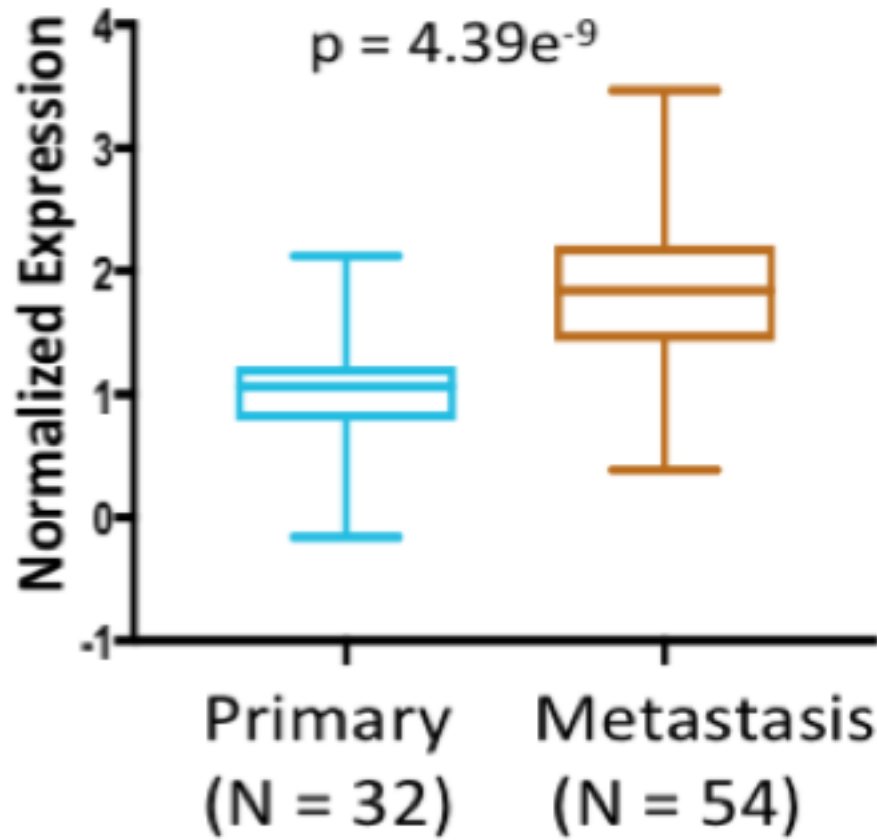


Fig 3. UCHL5 is overexpressed in metastatic melanoma. Box plot showing UCHL5 expression in matched primary and metastatic melanoma tissues.

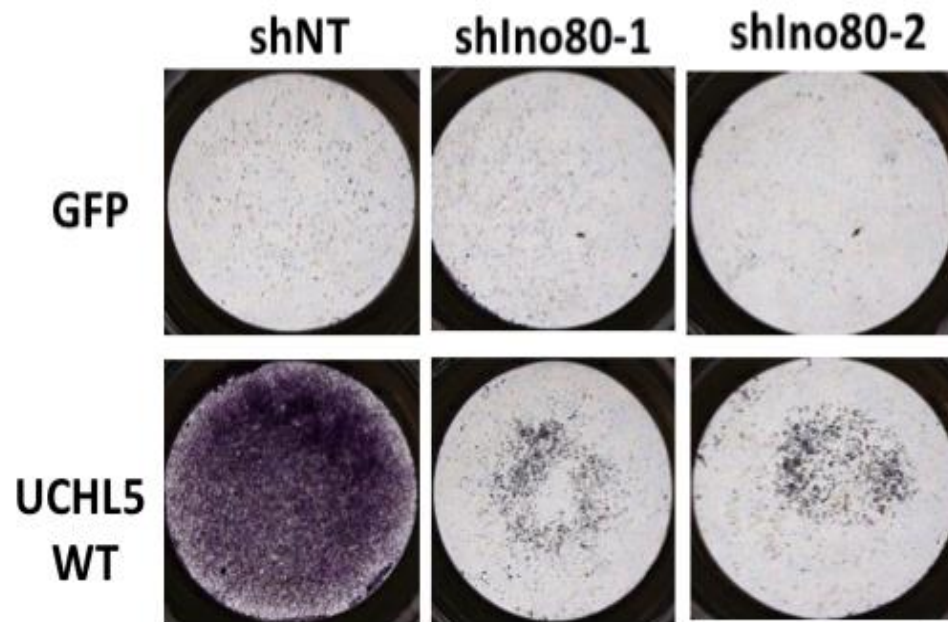


Fig 4. UCHL5 employs INO80 chromatin remodeling activity for promoting melanoma invasion. Images of invasive cells from Boyden chamber assay of WM115 GFP control or UCHL5 overexpressing cells harboring either control (shNT) shRNAs or Ino80-specific shRNAs.

1.2.2 Summary, Hypothesis, and Specific Aims

While the prognosis for melanoma has improved with the advent of immune checkpoint blockade, the 5-year survival rate for metastatic melanoma is still very low [3]. However, combination therapies, including those that combine epigenetic therapy with immunotherapy, have shown promise [4]. Based on the results of our *in vivo* ORF screen and subsequent experiments, we've found that UCHL5 is a pro-metastatic epigenetic driver of melanoma and is also overexpressed in metastatic melanoma (Fig 1-4). We hypothesize that UCHL5 promotes metastasis via epigenome reprogramming and its knockdown can alter melanoma progression and therapeutic response. The specific aims of this project are:

- 1) Identify mechanisms of UCHL5 action in metastasis.
- 2) Test contribution of UCHL5 to immune checkpoint therapy response.

Aim 1 will be carried out *in vitro* by knocking down UCHL5 in human metastatic melanoma cells, followed by ATAC-seq and ChIP-seq to determine involvement of the epigenome.

Aim 2 will be carried out an *in vivo* study by first knocking down UCHL5 in a mouse metastatic melanoma cell line, followed by injection of these cells into C57BL/6J mice and treatment of mice with immunotherapy upon palpable tumor formation.

Chapter 2: Methods and Materials

2.1 Cell Lines

All melanoma cell lines used in this study were commercially obtained. The human melanoma cell lines include a primary cell line, WM115, and its corresponding metastatic cell line, WM266-4. These cell lines were cultured in Dulbecco's Modified Eagle Medium (DMEM) supplemented with 10% Fetal Bovine Serum (FBS) and 1% Penicillin-Streptomycin (P/S). The mouse metastatic melanoma cell line that was used was B16F10, which was cultured in Dulbecco's Modified Eagle Medium (DMEM)/Nutrient Mixture F-12 (DME/F12) supplemented with 10% Fetal Bovine Serum (FBS) and 1% Penicillin-Streptomycin. Cells were cultured in a humidified incubator set at 37°C with 5% CO₂.

2.2 Plasmid Preparation

Bacterial glycerol stocks for short hairpin RNAs (shRNA) encoded in the pLKO.1 vector backbone and targeting UCHL5, were purchased from Sigma Aldrich. We started with 10 shRNAs targeting human UCHL5, 5 shRNAs targeting mouse UCHL5, and 4 non-target control vectors. We also obtained bacterial glycerol stock for pL6_UCHL5 for UCHL5 overexpression. Bacteria from glycerol stocks were cultured on Luria Broth (LB) Agar plates with carbenicillin, overnight. Single colonies were selected and cultured overnight in Terrific Broth and 100µg/ml working concentration of ampicillin. Bacterial culture was harvested at 4°C by centrifugation at 6000g, for 15 minutes. Plasmid DNA was purified using Qiagen Plasmid Maxi kit, and the concentration and purity of the DNA were measured using Nanodrop.

2.3 Lipid-based Transfection and Lentivirus Generation

Early passage Human Embryonic Kidney (HEK) 293T cells were transfected with 6µg of either pLKO_UCHL5 or pL6_UCHL5 or non-target control vectors and 3µg each of psPax2 (2nd generation lentiviral packaging plasmid) and pCMV_VSVG (envelope protein), along with Lipofectamine 3000, to generate lentivirus. Cells were maintained in OptiMEM during transfection. Media was changed to complete DMEM 7 hours after transfection. Lentiviral supernatant was collected 48 hours post-transfection, filtered using a 0.45 µm filter, and frozen at -80°C. Lentiviral titer was measured using abcam's qPCR lentivirus titer kit.

2.4 Generation of UCHL5 Knockdown and Overexpression Cell Lines

Lentiviral particles containing human pLKO_UCHL5 vectors and pL6_UCHL5 vectors were transduced into WM266-4 and WM115, respectively, along with 10µg/ml working concentration of polybrene transfection reagent. Lentiviral particles containing mouse pLKO_UCHL5 were transduced into B16F10 cells along with polybrene. Lentiviral particles containing non-target controls were also transduced into all 3 cell lines. Transduction was stopped after 20 hours, and antibiotic selection was initiated using 2µg/ml working concentration of puromycin or blasticidin for pLKO and pL6 vectors, respectively. Transduced WM266-4 and B16F10 cells were selected within 48 hours, when all control WM266-4 and B16F10 cells had died. Transduced WM115 cells were selected within 11 days when all control WM115 cells had died.

2.5 Western Blotting

WM266-4, WM115, and B16F10 cell lines growing in culture were washed with PBS, and trypsinized using 0.25% Trypsin. Whole cell lysates were prepared by resuspending the cells in an ice-cold RIPA buffer containing protease and

phosphatase inhibitors, keeping the cells on ice for 30 minutes, and collecting the supernatant at 4°C by centrifugation at 14,000 RPM for 15 minutes. Protein concentration was measured using the Pierce BCA protein assay kit, and quantified using Omega plate reader. Proteins were denatured by adding β -mercaptoethanol and boiling at 95°C for 10 minutes. Proteins were separated using an SDS-PAGE gel and transferred to a nitrocellulose membrane. Primary antibodies were diluted 1:1000 using non-fat dry milk or Bovine Serum Albumin (BSA) dissolved in Tris-buffered saline with 0.1% Tween 20 (TBST). Membranes containing proteins were incubated overnight in primary antibodies.

2.6 RNA-Sequencing

Cells were harvested from WM266-4 shNT-1, WM266-4 shUCHL5-1, and WM266-4 shUCHL5-4 cell culture dishes by washing the cells with PBS and trypsinizing with 0.25% Trypsin. Total RNA was extracted using Qiagen RNeasy Mini kit. β -mercaptoethanol was added to remove any ribonucleases. DNase treatment was done to remove any DNA. Concentration and purity of the eluted RNA were measured using Nanodrop. RNA degradation (RIN) was measured on TapeStation using High Sensitivity RNA ScreenTape Assay. Library preparation and sequencing were done at Novogene in Sacramento, California.

2.7 ATAC-Sequencing

Cells were harvested from WM266-4 shNT-1, WM266-4 shUCHL5-1, and WM266-4 shUCHL5-4 cell culture dishes by washing with PBS and trypsinizing with 0.25% Trypsin. Cell pellets were collected, washed with PBS, and frozen at -80°C. ATAC was done by following the ATAC-sequencing protocol from the Greenleaf lab

[36]. Sequencing was done using Illumina's NextSeq500 instrument at MD Anderson's Advanced Technology Genomics Core (ATGC) Laboratory.

2.8 ChIP-Sequencing

Cells were harvested from WM266-4 shNT-1 and WM266-4 shUCHL5-1 cell culture dishes by washing with PBS and trypsinizing with 0.25% Trypsin. ChIP was done by following the protocol from the Rai lab [37]. Library preparation was done by following the NEBNext Ultra II DNA Library Prep protocol. Quality control of DNA was done using Qubit and TapeStation. Sequencing was done using Illumina's NextSeq 500 instrument at MD Anderson's Advanced Technology Genomics Core Laboratory.

2.9 Mice

12 - 13 week old female C57BL/6J mice, purchased from The Jackson Laboratory, were used in this study. Mice were housed at MD Anderson's South Campus Vivarium, and animal experiments were conducted in accordance with the rules and regulations of The University of Texas MD Anderson Cancer Center Institutional Animal Use and Care Committee (IACUC).

2.10 Mouse Experiments

B16F10 shNT-1 and B16F10 shUCHL5-1 cell lines were used for mouse experiments. Cells from each line were resuspended in non-reduced Matrigel diluted 1:4 with PBS. Mice were injected subcutaneously with 100,000 cells of either B16F10 shNT-1 or B16F10 shUCHL5-1 cell line. Tumors were measured with a digital caliper. When tumors were palpable, mice were injected intraperitoneally with 100ug of either rat IgG2a isotype control or anti-mouse PD1 every other day until mice were moribund

and had to be euthanized. Mice were sacrificed, and tumor, spleen, liver, lungs, and draining lymph nodes were collected from mice and fixed using formalin for histology. Spleen and one chunk of tumor were processed for flow cytometry. One chunk of tumor was flash frozen for downstream applications.

2.11 Flow Cytometry

Cells were harvested from mouse tumors and spleens, and single cell suspensions were prepared using ice-cold PBS containing 1% FBS. Fluorescently labeled antibodies were added to single cell suspensions and incubated for 30 minutes at 4°C, away from light. After incubation, cells were washed, centrifuged, and supernatant was discarded. Cells were resuspended in 2% formaldehyde, and stored at 4°C, away from light, prior to flow cytometry. Flow cytometry was done for 4 panels, with compensation (Table 1).

Panel 1	Panel 2	Panel 3	Panel 4
CD45-BV711	CD45-BV711	CD45-BV711	CD45-BV711
Ly6G-BV421	CD3-BV421	CD62L-BV421	MHCII-BV421
CD103-PE	CD4-PE	CD44-PE	CD11b-APC
CD11b-APC	CD335-APC	CD4-FITC	CD206-FITC
MHCI-FITC CD11c-Percp	KLRG1-FITC NK1.1-Percp	Tim-3-Percp CD8a-AF700	CD11c-Percp CD86-AF700
CD8a-AF700	CXCR5-APCcy7	PD-1- PECF594	CD80-APCcy7
Ly6C-APCcy7	PD-1- PECF594	LAG-3-BV785	F4/80-Pecy7
F4/80-Pecy7	Live/dead BV510	Live/dead BV510	B220- PECF594
Gr-1-PE CF594		CTLA-4 PE CY7	PD-L1- BV785
Live/dead BV510			

Table 1. Panels run for flow cytometry.

2.12 Statistical Analysis

Microsoft Excel was used to document mouse tumor measurements and calculate tumor volume. GraphPad Prism was used for statistical analysis of experimental data. The two-way ANOVA test was used to compare the average tumor volumes of each of the 4 treatment groups. p values < 0.05 were considered statistically significant.

Chapter 3: Results

3.1 UCHL5 knockdown *in vitro* alters chromatin accessibility and promotes enhancer/super-enhancer reprogramming in metastatic melanoma.

We investigated the role of UCHL5 in metastatic melanoma by first knocking down UCHL5 in WM266-4, a human metastatic melanoma cell line. The reduction in expression was confirmed by Western Blotting (Fig 5A, B). We repeated the Western Blot to confirm knockdown in WM266-4 shUCHL5-1 (Fig 5B), as the loading control was not sufficient during the first attempt (Fig 5A).

To determine the role of UCHL5 in the epigenome, we performed ATAC-seq and ChIP-seq. The purpose of ATAC-seq is to determine chromatin accessibility by inserting hyperactive Tn5 transposase into open regions of the chromatin [36,38]. We found that UCHL5 knockdown alters accessibility on promoters and distal intergenic regions (enhancers) (Fig 6A). Specifically, we found that accessibility is increased in the promoter region and accessibility is decreased in the enhancer region. The signal around the TSS region may have been altered (Fig 6B). Unique sites were identified for both WM266-4 shNT-1 and WM266-4 shUCHL5-4, as well as pathways that were altered, including ones that are involved in interferon signaling and interferon gamma (Fig 6C). Various transcription factors were also affected by UCHL5 knockdown (Fig 6D). Since it's known that INO80 alters super-enhancers in melanoma [39], we wanted to determine whether UCHL5 also alters super-enhancers. ChIP-seq was done to determine whether UCHL5 is involved in enhancer and super-enhancer reprogramming. The purpose of ChIP-seq is to identify DNA-protein interactions and their binding sites [37,40]. We targeted

H3K27ac, a marker for active enhancer activity [41]. The ROSE algorithm was used to distinguish enhancers from super-enhancers during ChIP-sequencing data analysis [42]. Interestingly, we found that enhancers and super-enhancers were increased when UCHL5 is knocked down (Fig 7A, B). We also found various pathways, including the YAP1-ECM and EMT pathways to be enriched following UCHL5 knockdown (Fig 7C).

Since we identified some mesenchymal transcription factors through ATAC-seq (Fig 6D), we were interested in determining whether the protein expression of mesenchymal markers was also modified by UCHL5 knockdown. We looked at various mesenchymal markers and found that the expression of Vimentin and Snail is almost completely eliminated when UCHL5 is knocked down in WM266-4 (Fig 8A, B). However, the expression of Slug is increased following UCHL5 knock down (Fig 8C).

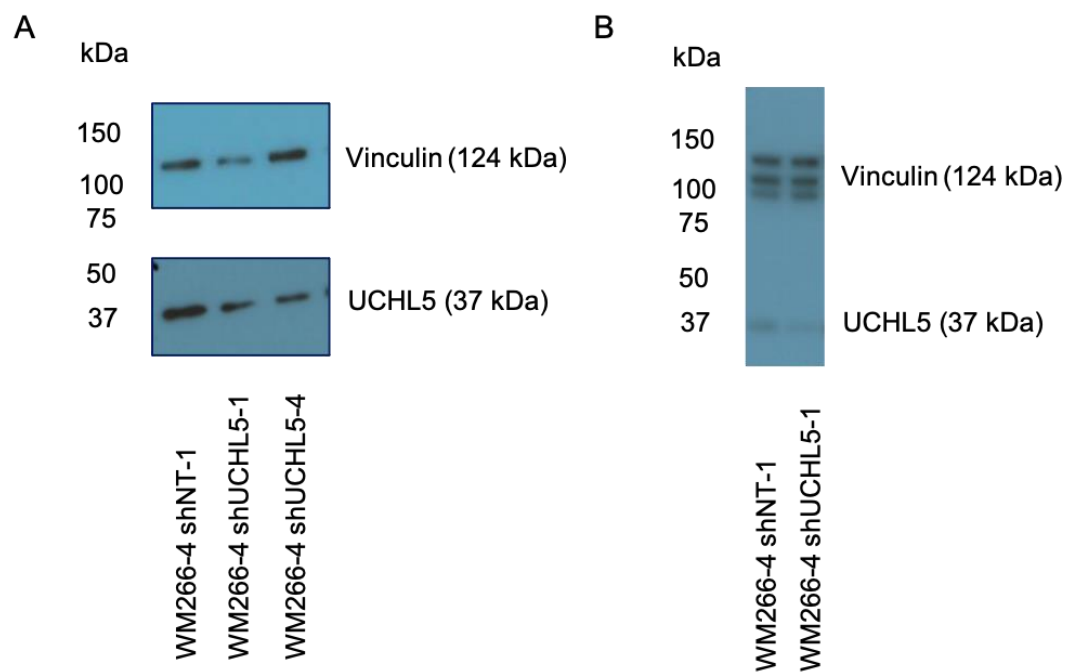


Fig 5. Confirmation of UCHL5 knockdown in WM266-4 by Western Blotting.

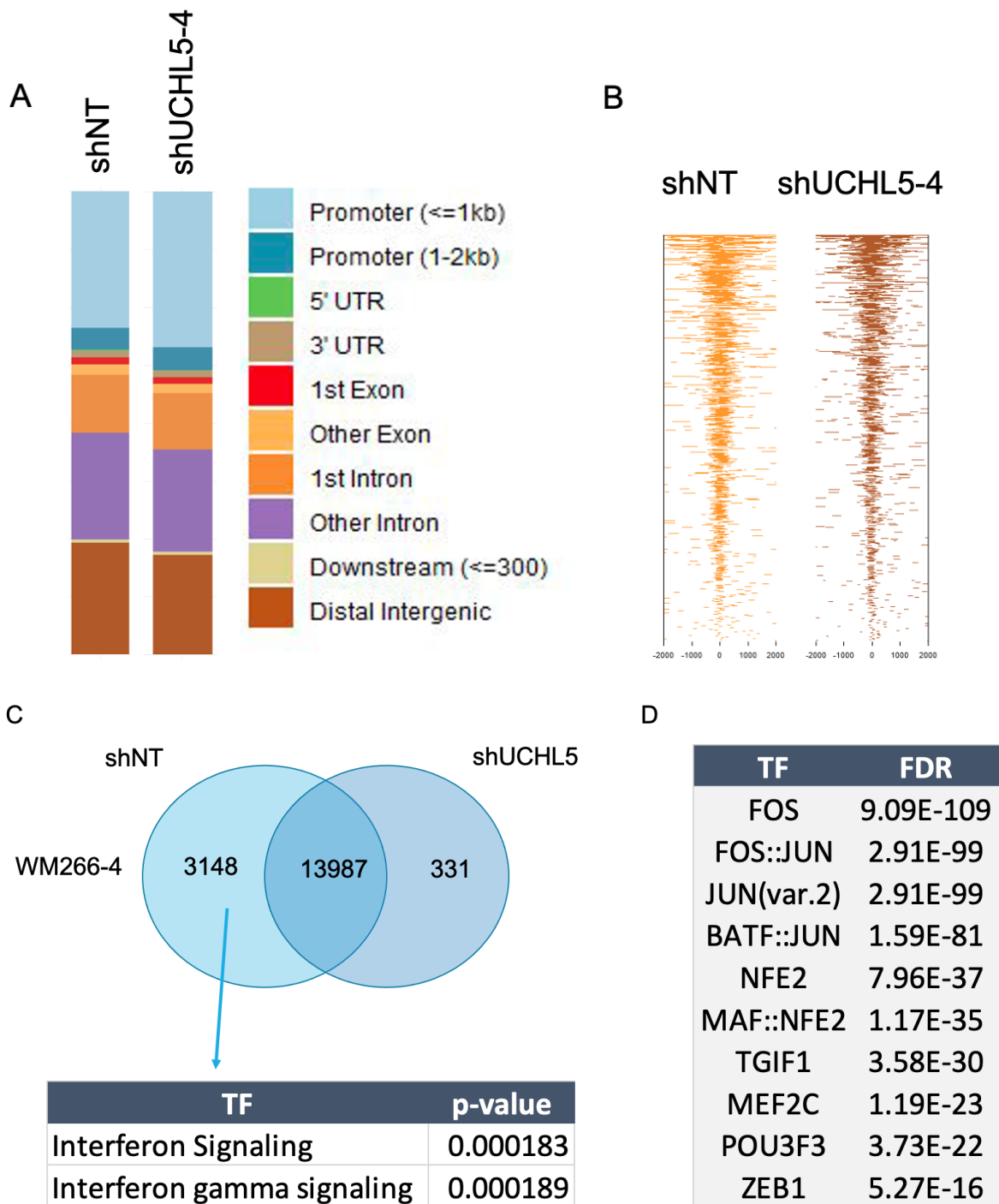


Fig 6. ATAC-seq shows UCL5 knockdown alters accessibility in regulatory regions. (A) Promoters and enhancers are altered. (B) Signal around the TSS doesn't appear altered. (C) Pathways and (D) transcription factors are altered.

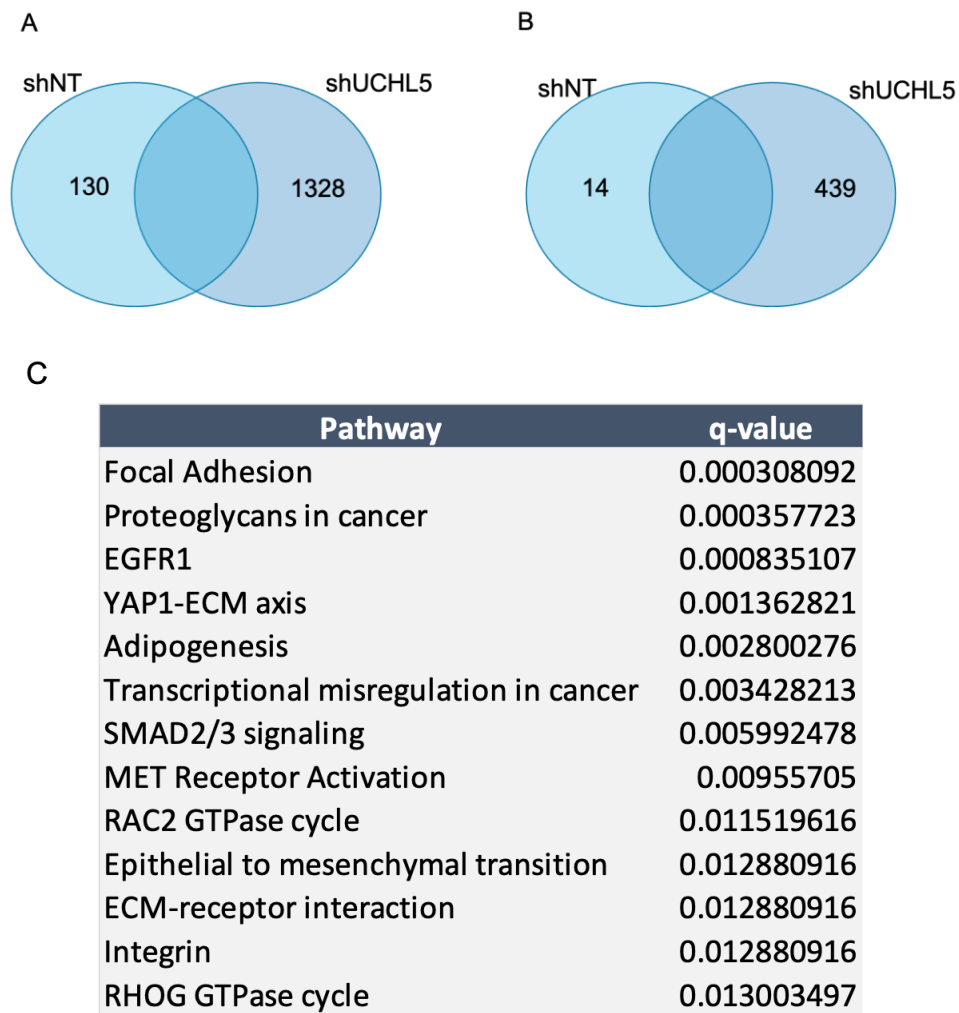


Fig 7. ChIP-seq reveals that UCHL5 knockdown promotes enhancer/super-enhancer reprogramming. (A) Enhancers and, (B) super-enhancers are reprogrammed following UCHL5 knockdown. (C) Super-enhancer alterations impact several pathways.

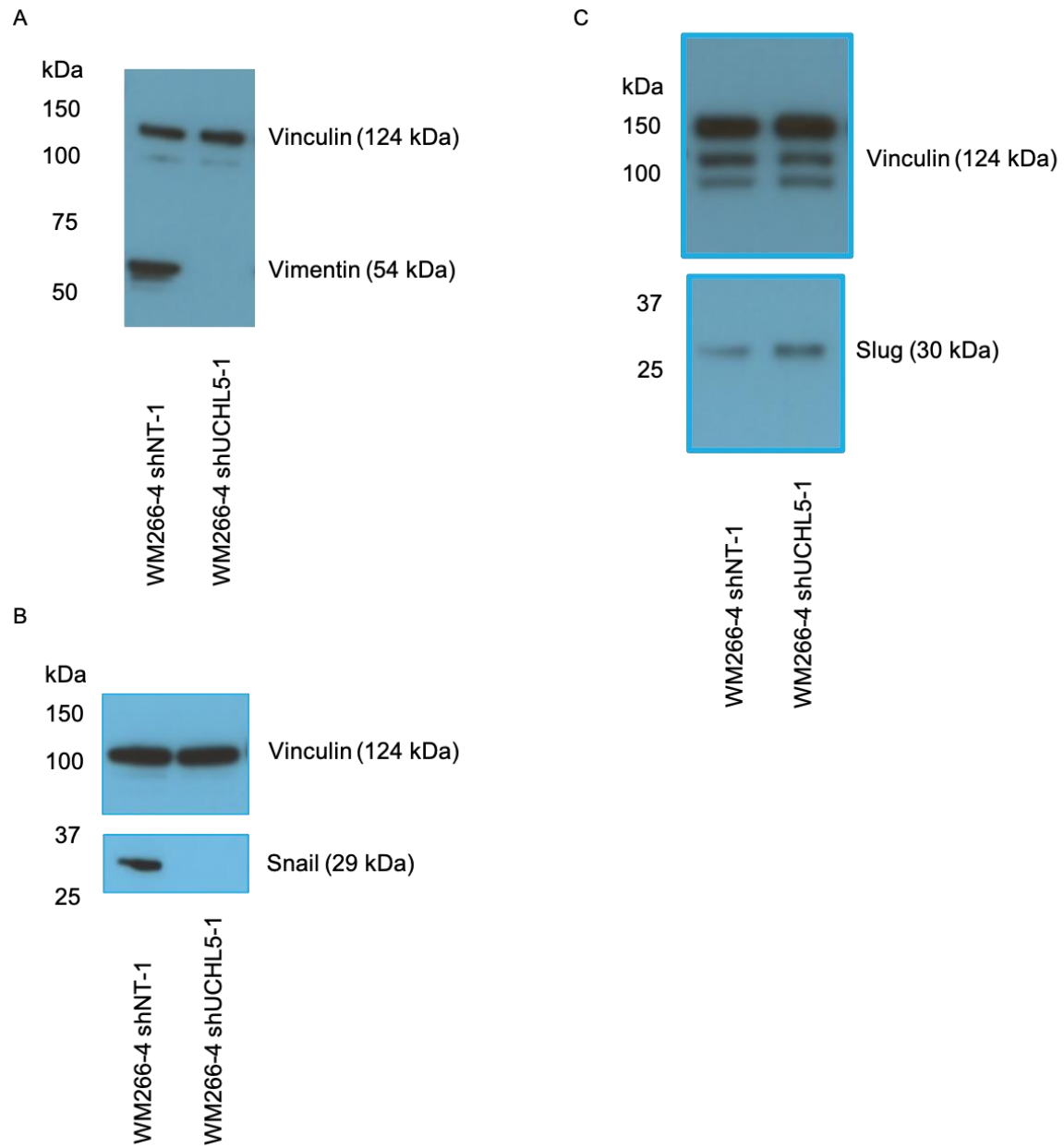


Fig 8. UCL5 knockdown alters mesenchymal gene expression. Expression is altered for A) Vimentin, B) Snail, C) Slug.

3.2 UCHL5 knockdown combined with anti-PD1 treatment increases tumor burden in mice.

There are currently 2 major unmet clinical needs, including 1) combination therapies to increase response rate, and 2) biomarkers for response. Immune checkpoint blockade has shown success over the past decade and works by stopping the interaction between cancer cells and cytotoxic T cells at immune checkpoints [43]. The interaction between programmed cell-death ligand 1 (PDL-1) on the surface of cancer cells and programmed cell-death 1 (PD-1) on the surface of cytotoxic T cells prevents T cells from attacking cancer cells [43]. Melanoma patients treated with anti-PD1 have shown an objective response rate of 30%-40% [44], but there is still room for improvement with combination therapies [45].

DNA damage repair and chromatin remodeling are considered 2 of the determinants of immunotherapy response [46]. The INO80 chromatin remodeling complex interacts with UCHL5 and is known to play a role in DNA damage repair and genome stability [47]. We have also found that knocking down UCHL5 alters chromatin accessibility on regulators of interferon signaling (Fig 6C). Therefore, we are interested in determining whether UCHL5 blockade in combination with anti-PD1 can be an effective treatment for metastatic melanoma.

To test the contribution of UCHL5 to immune checkpoint therapy response, we first knocked down UCHL5 in B16F10, a mouse metastatic melanoma cell line. We selected B16F10 shNT-1 as our non-targeting control, and B16F10 shUCHL5-1 as the knocked down cell line, after UCHL5 expression was probed in various B16F10 shNT and B16F10 shUCHL5 cell lines, by western blotting (Fig 9).

Next, we did an *in vivo* study where we looked at the effect of different treatments on tumor burden (Fig 10). 100,000 cells of either B16F10 shNT-1 or B16F10 shUCHL5-1, were injected subcutaneously into 20 x C57BL/6J female mice. Treatment with anti-mouse PD1 or Isotype control began when tumors were palpable, resulting in a total of 4 treatment groups (B16F10 shNT-1 IgG, B16F10 shNT-1 anti-PD1, B16F10 shUCHL5-1 IgG, and B16F10 shUCHL5-1 anti-PD1). Lungs, liver, lymph nodes, spleen, and tumor were harvested after mice were sacrificed due to moribund condition. Treatment with anti-PD1 decreased tumor burden in the B16F10 shNT-1 anti-PD1 group, when compared to the B16F10 shNT-1 IgG group (Fig 11). The B16F10 shUCHL5-1 IgG group had the smallest tumor burden, and this was statistically significant when compared to the B16F10 shNT-1 IgG group. Interestingly, the B16F10 shUCHL5-1 anti-PD1 group had the greatest tumor burden. This was statistically significant when compared to the B16F10 shNT-1 anti-PD1 and B16F10 shUCHL5-1 IgG groups, but not the B16F10 shNT-1 IgG group. Mice in the 2 B16F10 shNT-1 groups were the first to develop tumors. However, the B16F0 shUCHL5-1 anti-PD1 group's tumor growth was accelerated during treatment.

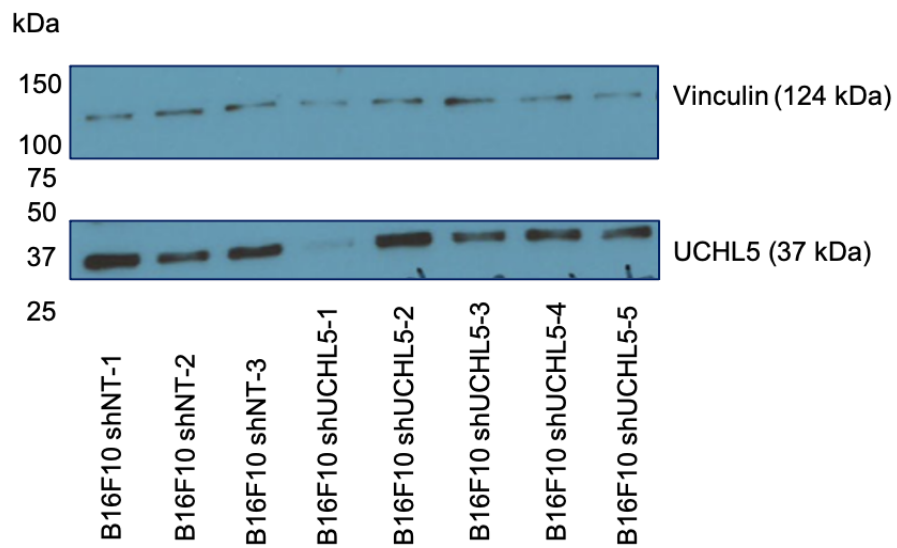


Fig 9. Validation of UCHL5 knockdown in B16F10 mouse melanoma cell lines.

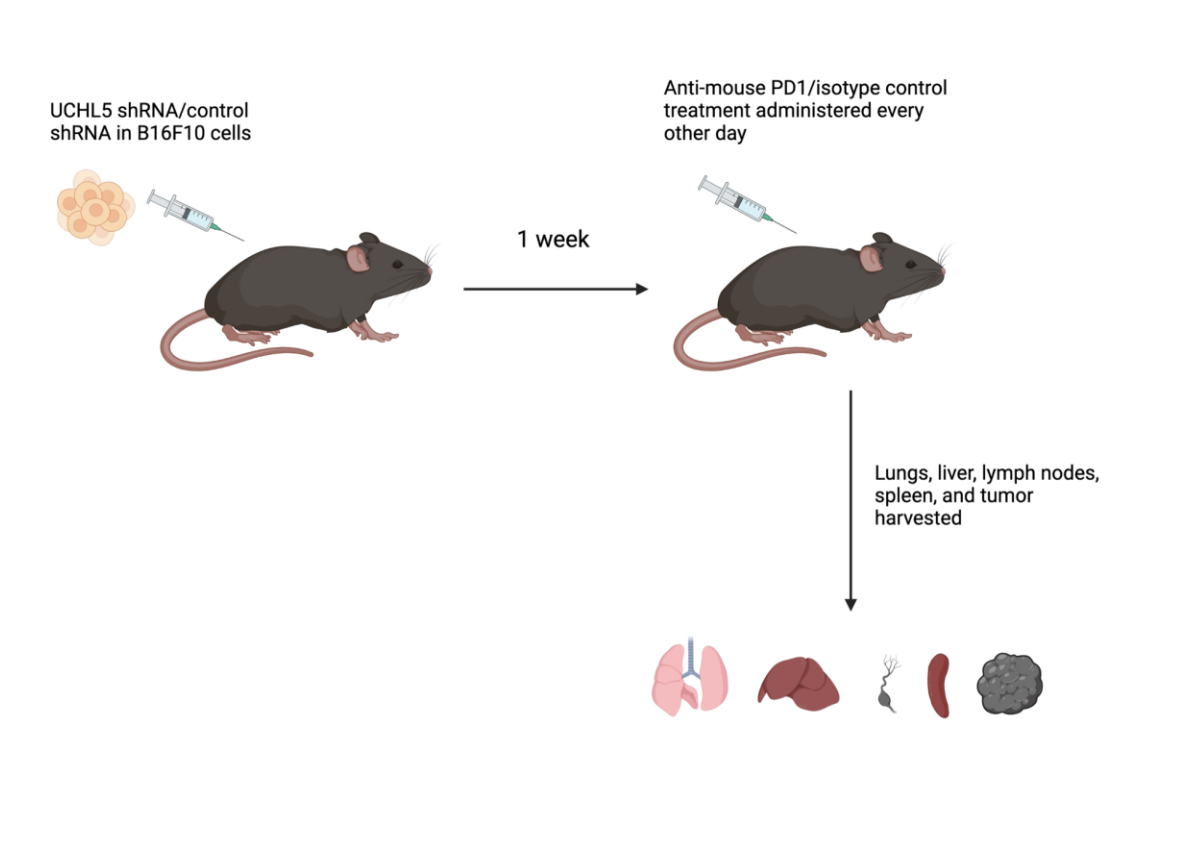


Fig 10. Schematic of mouse experiment. Mice were injected subcutaneously with either B16F10 shNT-1 or B16F10 shUCHL5-1 cells. Treatment with mouse anti-PD1 or isotype control began 1 week later when tumors were palpable. Mice were treated intraperitoneally every other day until mice were sacrificed due to moribund condition. Lungs, liver, lymph nodes, spleen, and tumor were harvested (figure created with BioRender.com).

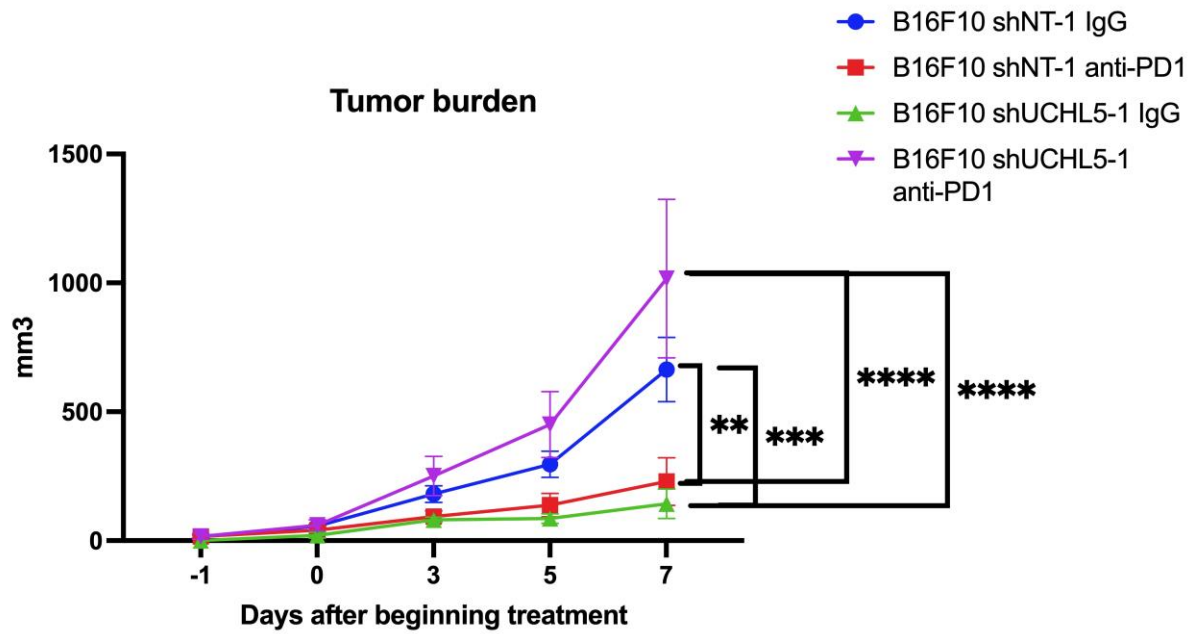


Fig 11. UCHL5 knockdown combined with anti-PD1 treatment increases tumor burden.

3.3 UCHL5 knockdown combined with anti-PD1 treatment may alter the immune microenvironment.

We were interested in determining whether combining UCHL5 knockdown with anti-PD1 therapy altered the immune microenvironment in response to treatment. We did immune profiling using flow cytometry and found that pre-exhausted and exhausted CD4+ and CD8+ T cells may be altered (Fig 12). The B16F10 UCHL5 KD + anti-PD-1 treatment group showed the smallest percent of exhausted CD8+ T cells, while the B16F10 NT1 +IgG group showed the greatest percent. CD4+ T cells, CD8+ T cells, naïve CD4 cells, effector CD4 cells, memory CD4 cells, naïve CD8 cells, effector CD8 cells, and memory CD8 cells, all appeared to be altered (Fig 13). There were fewer memory CD4 and CD8 cells for the B16F10 UCHL5 +anti-PD-1 group than for the B16F10 NT1 +IgG group. However, none of these results were statistically significant.

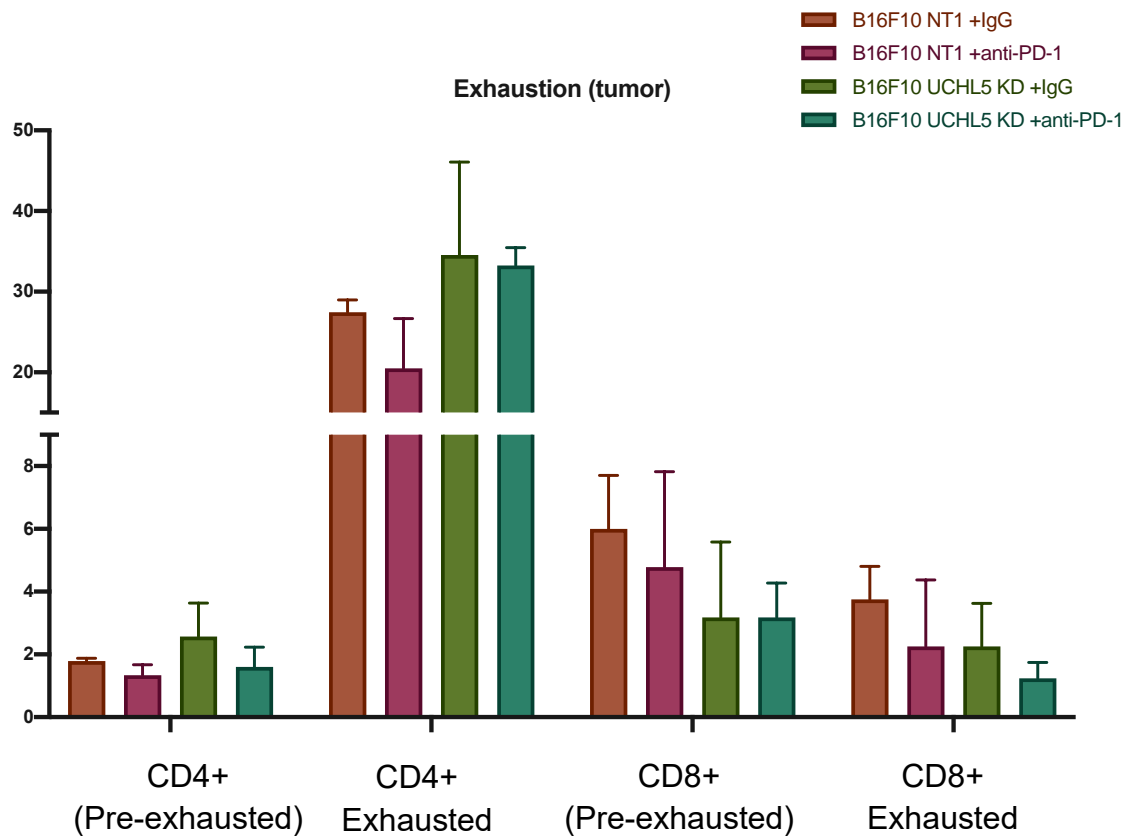


Fig 12. Exhausted T cells may be altered upon UCHL5 knockdown and PD1 blockade.

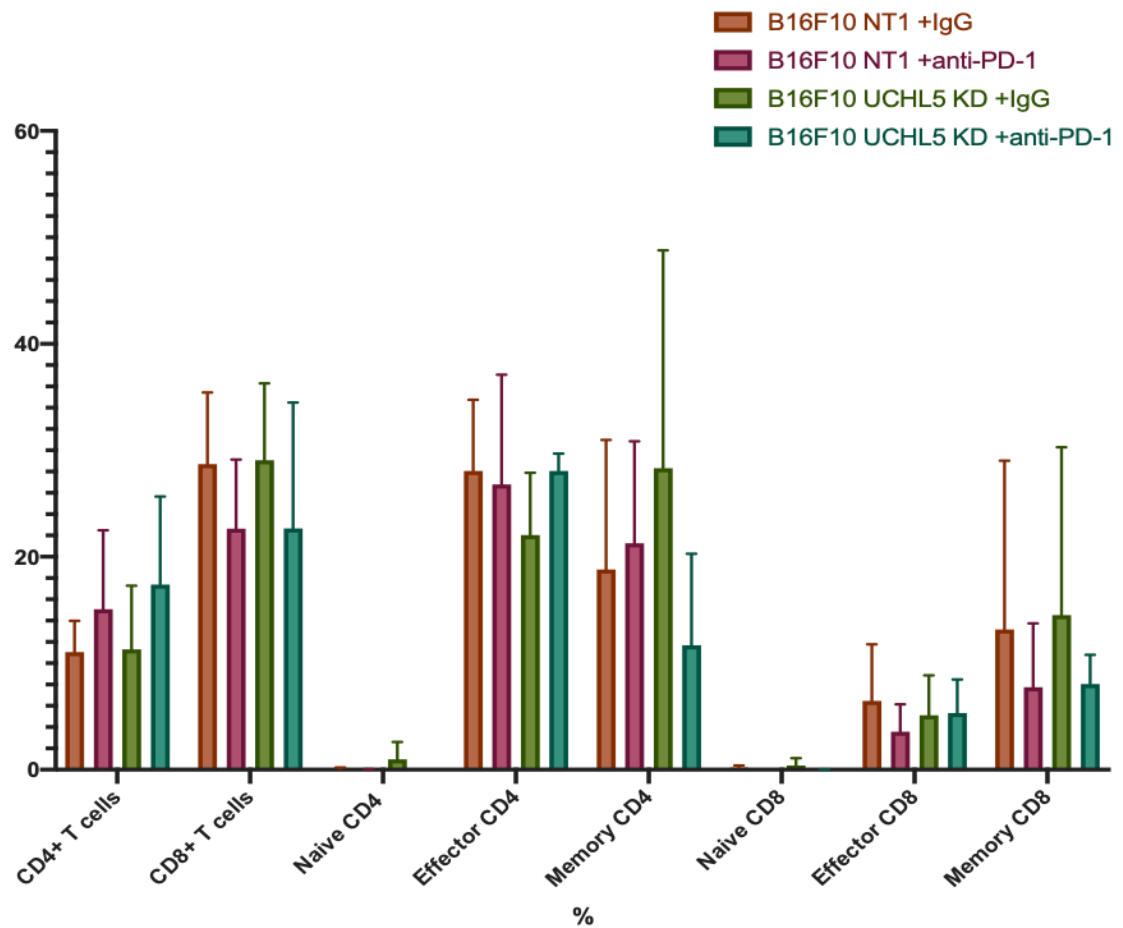


Fig 13. Memory T cells may be altered upon UCHL5 knockdown and PD1 blockade.

Chapter 4: Discussion, Future Directions, and Conclusions

4.1 Discussion

There is a gap of knowledge regarding epigenetic alterations driving cancer progression, including in melanoma. Since we have identified UCHL5 as a pro-metastatic epigenetic driver of melanoma, UCHL5 could be targeted to prevent metastatic progression. UCHL5 has also been identified as a candidate in an *in vitro* screen for pro-invasion oncogenes in primary melanoma [48]. It's known that UCHL5 interacts with the INO80 chromatin remodeling complex [9,15,16], and that INO80 also promotes melanoma tumorigenesis [49]. Here, we have shown that UCHL5 indeed employs INO80 to promote invasion in melanoma. We have 2 possible targets to prevent invasion. UCHL5 has been shown to be overexpressed in multiple cancers, and this overexpression of UCHL5 also leads to a worse prognosis in many of these cancers [12,13,14,27,28,29,30]. However, UCHL5 has not been well-characterized in either primary or metastatic melanoma, which was our motivation for investigating its role in metastatic melanoma.

ATAC-seq showed that UCHL5 knockdown alters different pathways, including the interferon signaling pathway. Regulators within this pathway were altered because of the change in chromatin accessibility. The interferon signaling pathway is complex and is involved in the immune response and a part of the innate immune system [50]. It could also play a role in modulating immunotherapy response. Pathways that were impacted by epigenome reprogramming included the YAP1-ECM pathway and the EMT pathway. The EMT pathway is known to play a crucial role in metastasis. This was consistent with the altered expression that we saw for mesenchymal markers

including Vimentin, Snail, and Slug. Normal functions of YAP1 include regulating gene expression and cell proliferation [51]. We have previously found that YAP1 interacts with UCHL5 (Fig 14). YAP1 is also involved in facilitating metastasis through the EMT process [51]. YAP1 has also been shown to regulate ARHGAP29 and drive metastasis through the Rho-cofilin-LIMK signaling [52].

There is evidence that combining therapies that target the genome/epigenome and immune checkpoints, generates a stronger response against the tumor [4]. However, our *in vivo* study has shown the opposite result. A recent publication from Eschweiler et al., suggests that treatment with anti-CTLA-4 prior to treating with anti-PD1 depletes follicular regulatory T cells, resulting in a strong anti-tumor response where prior monotherapy was ineffective [53]. This, however, doesn't explain the worsened tumor burden following combination therapy. We do know that anti-PD1 treatment works in the B16F10 cell line because the B16F10 shNT-1 anti-PD1 treatment group had a smaller tumor burden compared to the B16F10 shNT-1 IgG group following treatment. It should also be noted that UCHL5 knockdown alone is effective at decreasing tumor burden, as seen in the B16F10 shUCHL5-1 IgG group. Monotherapy in this case was effective while combination therapy failed. The B16F10 shUCHL5-1 anti-PD1 group had the lowest percentage of exhausted CD8+ T cells. In theory, this group should have been able to fight the cancer and reduce tumor burden because CD8+ T cells should have been functional. However, this was not the case. It is known that one of the normal functions of UCHL5 is DNA repair through double-strand end break resection and homologous recombination [25]. Knocking down UCHL5 could have interfered with DNA double-strand break (DSB) repair. It has been

shown that PDL-1 can be upregulated in response to DSB [54]. This provides a possible explanation for why the combination of UCHL5 blockade and anti-PD1 therapy may have caused an increased tumor burden in the mice. It would be interesting to see the effect of a UCHL5 inhibitor such as b-AP15, combined with anti-PD1 therapy, as opposed to knocking down UCHL5 using shRNAs. b-AP15 has been shown to target UCHL5 in Waldenstrom Macroglobulinemia, a rare and incurable non-Hodgkin's lymphoma [30].

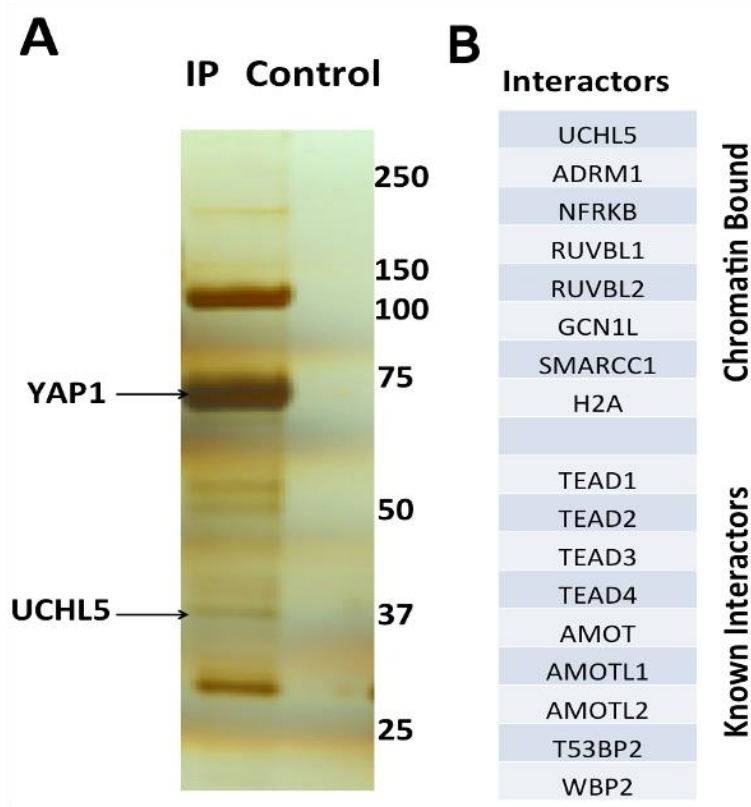
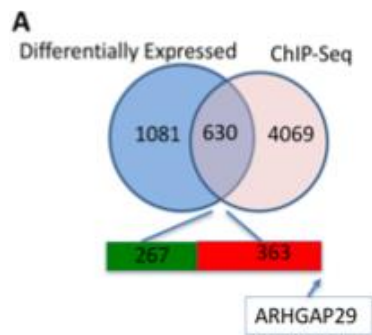


Fig 14. UCHL5 interacts with YAP1. A) UCHL5 was co-precipitated with YAP1. B) List of proteins that interact with YAP1.

4.2 Future Directions

1) Our lab previously found ARHGAP29 to be a direct target of UCHL5, by performing RNA-seq and ChIP-seq in WM115 cells expressing FLAG-tagged UCHL5 (Fig 15A). The 630 genes that were identified were enriched in transcription, kinase signaling, axon guidance, apoptosis, and actin cytoskeleton reorganization (Fig 15B). We are therefore interested in investigating how UCHL5 regulates ARHGAP29. We are currently creating modified melanoma cell lines which we plan to inject into mice. This includes overexpressing ARHGAP29 in a WM266-4 cell line where UCHL5 has been knocked down. We are also knocking down ARHGAP29 in a WM115 cell line where UCHL5 is overexpressed. Once ARHGAP29 expression levels are confirmed, we will do tail vein injections in mice to check for metastases.

2) Since we observed an increased tumor burden after the combination UCHL5 blockade and anti-PD1 therapy, we are interested in finding out what caused this outcome. We plan on investigating the underlying mechanism by looking at whether UCHL5 knockdown induces DSB related pathways and causes an upregulation of PD-L1.



B

Term	FDR
Regulation of transcription	2.0E-03
Regulation of protein kinase signaling	2.5E-03
Axon Guidance	3.1E-03
Negative regulation of apoptosis	3.9E-03
actin cytoskeleton organization	7.6E-03

Fig 15. Overlap of UCHL5-occupied genes and differential gene expression shows ARHGAP29 as a UCHL5 target.

4.3 Conclusions

In this project, we have shown that UCHL5 knockdown alters chromatin accessibility and promotes epigenomic reprogramming in metastatic melanoma. As a result, various pathways are impacted, including a few that are involved in metastasis and the immune response. UCHL5 knockdown also alters mesenchymal gene expression, including that of genes that are canonically known to be involved in EMT. Targeting metastatic melanoma with UCHL5 blockade and anti-PD1 therapy leads to an increased tumor burden. We have shown that UCHL5 interacts with INO80 and also promotes epigenomic reprogramming, and UCHL5 could theoretically regulate ARHGAP29 through the Rho-cofilin-LIMK pathway to promote invasion and metastasis (Fig 16). The latter remains to be elucidated. Elucidating more components of this pathway could provide more opportunities to target proteins that are involved in invasion and metastasis. These findings can provide insight into how we approach treatment for metastatic melanoma, including how we target and modulate the function of UCHL5.

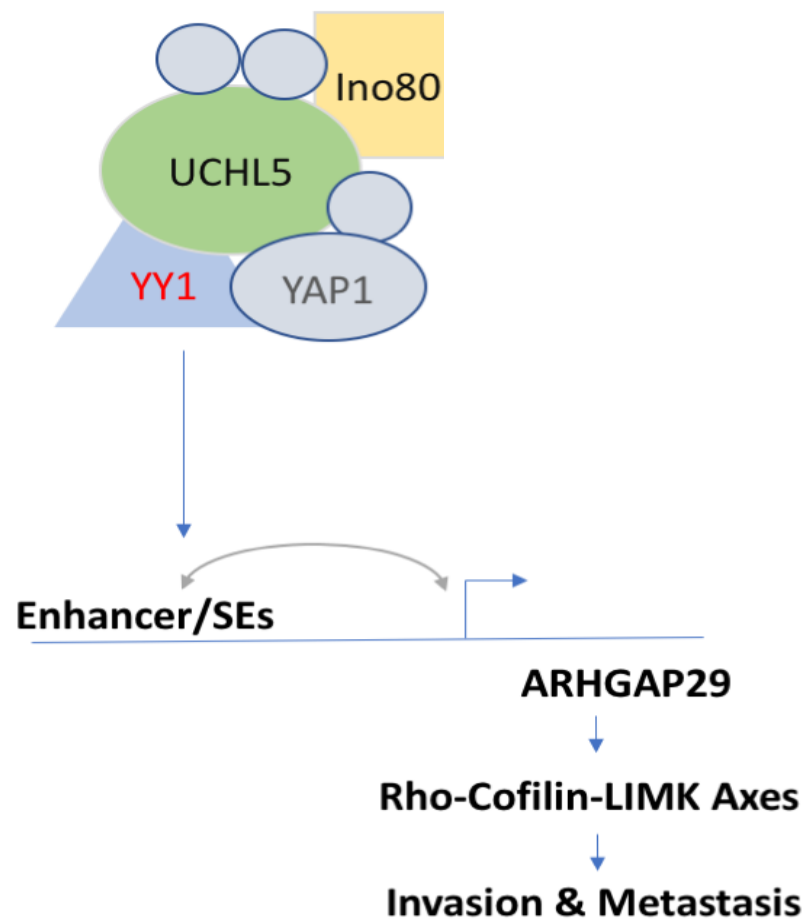


Fig 16. Model of UCHL5 interactions, regulatory functions, and downstream targets.

Bibliography

1. Tampa, M., Georgescu, S. R., Mitran, M. I., Mitran, C. I., Matei, C., Caruntu, A., Scheau, C., Nicolae, I., Matei, A., Caruntu, C., Constantin, C., & Neagu, M. (2021). Current Perspectives on the Role of Matrix Metalloproteinases in the Pathogenesis of Basal Cell Carcinoma. *Biomolecules*, 11(6), 903.
<https://doi.org/10.3390/biom11060903>
2. Steininger, J., Gellrich, F. F., Schulz, A., Westphal, D., Beissert, S., & Meier, F. (2021). Systemic Therapy of Metastatic Melanoma: On the Road to Cure. *Cancers*, 13(6), 1430. <https://doi.org/10.3390/cancers13061430>
3. Villani, A., Scalvenzi, M., Fabbrocini, G., Ocampo-Candiani, J., & Ocampo-Garza, S. S. (2021). Looking into a Better Future: Novel Therapies for Metastatic Melanoma. *Dermatology and therapy*, 11(3), 751–767.
<https://doi.org/10.1007/s13555-021-00525-9>
4. Martinez-Useros, J., Martin-Galan, M., Florez-Cespedes, M., & Garcia-Foncillas, J. (2021). Epigenetics of Most Aggressive Solid Tumors: Pathways, Targets and Treatments. *Cancers*, 13(13), 3209.
<https://doi.org/10.3390/cancers13133209>
5. Elshiaty, M., Schindler, H., & Christopoulos, P. (2021). Principles and Current Clinical Landscape of Multispecific Antibodies against Cancer. *International journal of molecular sciences*, 22(11), 5632.
<https://doi.org/10.3390/ijms22115632>

6. Lam, Y. A., Xu, W., DeMartino, G. N., & Cohen, R. E. (1997). Editing of ubiquitin conjugates by an isopeptidase in the 26S proteasome. *Nature*, 385(6618), 737–740. <https://doi.org/10.1038/385737a0>
7. Yao, T., Song, L., Xu, W., DeMartino, G. N., Florens, L., Swanson, S. K., Washburn, M. P., Conaway, R. C., Conaway, J. W., & Cohen, R. E. (2006). Proteasome recruitment and activation of the Uch37 deubiquitinating enzyme by Adrm1. *Nature cell biology*, 8(9), 994–1002. <https://doi.org/10.1038/ncb1460>
8. Wicks, S. J., Haros, K., Maillard, M., Song, L., Cohen, R. E., Dijke, P. T., & Chantry, A. (2005). The deubiquitinating enzyme UCH37 interacts with Smads and regulates TGF-beta signalling. *Oncogene*, 24(54), 8080–8084. <https://doi.org/10.1038/sj.onc.1208944>
9. Vander Linden, R. T., Hemmis, C. W., Schmitt, B., Ndoja, A., Whitby, F. G., Robinson, H., Cohen, R. E., Yao, T., & Hill, C. P. (2015). Structural basis for the activation and inhibition of the UCH37 deubiquitylase. *Molecular cell*, 57(5), 901–911. <https://doi.org/10.1016/j.molcel.2015.01.016>
10. Burgie, S. E., Bingman, C. A., Soni, A. B., & Phillips, G. N., Jr (2012). Structural characterization of human Uch37. *Proteins*, 80(2), 649–654. <https://doi.org/10.1002/prot.23147>
11. Li, Z., Zhou, L., Jiang, T., Fan, L., Liu, X., & Qiu, X. (2019). Proteasomal deubiquitinase UCH37 inhibits degradation of β -catenin and promotes cell proliferation and motility. *Acta biochimica et biophysica Sinica*, 51(3), 277–284. <https://doi.org/10.1093/abbs/gmy176>

12. Tian, Z., D'Arcy, P., Wang, X., Ray, A., Tai, Y. T., Hu, Y., Carrasco, R. D., Richardson, P., Linder, S., Chauhan, D., & Anderson, K. C. (2014). A novel small molecule inhibitor of deubiquitylating enzyme USP14 and UCHL5 induces apoptosis in multiple myeloma and overcomes bortezomib resistance. *Blood*, 123(5), 706–716. <https://doi.org/10.1182/blood-2013-05-500033>
13. Fang, Y., & Shen, X. (2017). Ubiquitin carboxyl-terminal hydrolases: involvement in cancer progression and clinical implications. *Cancer metastasis reviews*, 36(4), 669–682. <https://doi.org/10.1007/s10555-017-9702-0>
14. Zhang, J., Xu, H., Yang, X., Zhao, Y., Xu, X., Zhang, L., Xuan, X., Ma, C., Qian, W., & Li, D. (2020). Deubiquitinase UCHL5 is elevated and associated with a poor clinical outcome in lung adenocarcinoma (LUAD). *Journal of Cancer*, 11(22), 6675–6685. <https://doi.org/10.7150/jca.46146>
15. Cai, Y., Jin, J., Yao, T., Gottschalk, A. J., Swanson, S. K., Wu, S., Shi, Y., Washburn, M. P., Florens, L., Conaway, R. C., & Conaway, J. W. (2007). YY1 functions with INO80 to activate transcription. *Nature structural & molecular biology*, 14(9), 872–874. <https://doi.org/10.1038/nsmb1276>
16. Yao, T., Song, L., Jin, J., Cai, Y., Takahashi, H., Swanson, S. K., Washburn, M. P., Florens, L., Conaway, R. C., Cohen, R. E., & Conaway, J. W. (2008). Distinct modes of regulation of the Uch37 deubiquitinating enzyme in the proteasome and in the Ino80 chromatin-remodeling complex. *Molecular cell*, 31(6), 909–917. <https://doi.org/10.1016/j.molcel.2008.08.027>

17. Dickson, P., Simanski, S., Ngundu, J. M., & Kodadek, T. (2020). Mechanistic Studies of the Multiple Myeloma and Melanoma Cell-Selective Toxicity of the Rpn13-Binding Peptoid KDT-11. *Cell chemical biology*, 27(11), 1383–1395.e5. <https://doi.org/10.1016/j.chembiol.2020.08.008>
18. Reddington, C. J., Fellner, M., Burgess, A. E., & Mace, P. D. (2020). Molecular Regulation of the Polycomb Repressive-Deubiquitinase. *International journal of molecular sciences*, 21(21), 7837. <https://doi.org/10.3390/ijms21217837>
19. de Poot, S., Tian, G., & Finley, D. (2017). Meddling with Fate: The Proteasomal Deubiquitinating Enzymes. *Journal of molecular biology*, 429(22), 3525–3545. <https://doi.org/10.1016/j.jmb.2017.09.015>
20. Sahtoe, D. D., van Dijk, W. J., El Oualid, F., Ekkebus, R., Ovaa, H., & Sixma, T. K. (2015). Mechanism of UCH-L5 activation and inhibition by DEUBAD domains in RPN13 and INO80G. *Molecular cell*, 57(5), 887–900. <https://doi.org/10.1016/j.molcel.2014.12.039>
21. Reyes-Turcu, F. E., Ventii, K. H., & Wilkinson, K. D. (2009). Regulation and cellular roles of ubiquitin-specific deubiquitinating enzymes. *Annual review of biochemistry*, 78, 363–397. <https://doi.org/10.1146/annurev.biochem.78.082307.091526>
22. Deol, K. K., Crowe, S. O., Du, J., Bisbee, H. A., Guenette, R. G., & Strieter, E. R. (2020). Proteasome-Bound UCH37/UCHL5 Debranches Ubiquitin Chains to Promote Degradation. *Molecular cell*, 80(5), 796–809.e9. <https://doi.org/10.1016/j.molcel.2020.10.017>

23. Lam, Y. A., DeMartino, G. N., Pickart, C. M., & Cohen, R. E. (1997). Specificity of the ubiquitin isopeptidase in the PA700 regulatory complex of 26 S proteasomes. *The Journal of biological chemistry*, 272(45), 28438–28446. <https://doi.org/10.1074/jbc.272.45.28438>
24. Randles, L., Anchoori, R. K., Roden, R. B., & Walters, K. J. (2016). The Proteasome Ubiquitin Receptor hRpn13 and Its Interacting Deubiquitinating Enzyme Uch37 Are Required for Proper Cell Cycle Progression. *The Journal of biological chemistry*, 291(16), 8773–8783. <https://doi.org/10.1074/jbc.M115.694588>
25. Nishi, R., Wijnhoven, P., le Sage, C., Tjeertes, J., Galanty, Y., Forment, J. V., Clague, M. J., Urbé, S., & Jackson, S. P. (2014). Systematic characterization of deubiquitylating enzymes for roles in maintaining genome integrity. *Nature cell biology*, 16(10), 1016–8. <https://doi.org/10.1038/ncb3028>
26. Al-Shami, A., Jhaver, K. G., Vogel, P., Wilkins, C., Humphries, J., Davis, J. J., Xu, N., Potter, D. G., Gerhardt, B., Mullinax, R., Shirley, C. R., Anderson, S. J., & Oravecz, T. (2010). Regulators of the proteasome pathway, Uch37 and Rpn13, play distinct roles in mouse development. *PloS one*, 5(10), e13654. <https://doi.org/10.1371/journal.pone.0013654>
27. Rolén, U., Kobzeva, V., Gasparjan, N., Ovaa, H., Winberg, G., Kissel'jov, F., & Masucci, M. G. (2006). Activity profiling of deubiquitinating enzymes in cervical carcinoma biopsies and cell lines. *Molecular carcinogenesis*, 45(4), 260–269. <https://doi.org/10.1002/mc.20177>

28. Fang, Y., Fu, D., Tang, W., Cai, Y., Ma, D., Wang, H., Xue, R., Liu, T., Huang, X., Dong, L., Wu, H., & Shen, X. (2013). Ubiquitin C-terminal Hydrolase 37, a novel predictor for hepatocellular carcinoma recurrence, promotes cell migration and invasion via interacting and deubiquitinating PRP19. *Biochimica et biophysica acta*, 1833(3), 559–572.
<https://doi.org/10.1016/j.bbamcr.2012.11.020>
29. Wang, L., Chen, Y. J., Xu, K., Wang, Y. Y., Shen, X. Z., & Tu, R. Q. (2014). High expression of UCH37 is significantly associated with poor prognosis in human epithelial ovarian cancer. *Tumour biology : the journal of the International Society for Oncodevelopmental Biology and Medicine*, 35(11), 11427–11433. <https://doi.org/10.1007/s13277-014-2446-3>
30. Chitta, K., Paulus, A., Akhtar, S., Blake, M. K., Caulfield, T. R., Novak, A. J., Ansell, S. M., Advani, P., Ailawadhi, S., Sher, T., Linder, S., & Chanan-Khan, A. (2015). Targeted inhibition of the deubiquitinating enzymes, USP14 and UCHL5, induces proteotoxic stress and apoptosis in Waldenström macroglobulinaemia tumour cells. *British journal of haematology*, 169(3), 377–390. <https://doi.org/10.1111/bjh.13304>
31. Kikuchi, M., Ogishima, S., Miyamoto, T., Miyashita, A., Kuwano, R., Nakaya, J., & Tanaka, H. (2013). Identification of unstable network modules reveals disease modules associated with the progression of Alzheimer's disease. *PloS one*, 8(11), e76162. <https://doi.org/10.1371/journal.pone.0076162>

32. Tímár, J., Vizkeleti, L., Doma, V., Barbai, T., & Rásó, E. (2016). Genetic progression of malignant melanoma. *Cancer metastasis reviews*, 35(1), 93–107. <https://doi.org/10.1007/s10555-016-9613-5>.
33. Davis, E. J., Johnson, D. B., Sosman, J. A., & Chandra, S. (2018). Melanoma: What do all the mutations mean?. *Cancer*, 124(17), 3490–3499. <https://doi.org/10.1002/cncr.31345>.
34. Yates, L. R., & Campbell, P. J. (2012). Evolution of the cancer genome. *Nature reviews. Genetics*, 13(11), 795–806. <https://doi.org/10.1038/nrg3317>
35. Xu, L., Shen, S. S., Hoshida, Y., Subramanian, A., Ross, K., Brunet, J. P., Wagner, S. N., Ramaswamy, S., Mesirov, J. P., & Hynes, R. O. (2008). Gene expression changes in an animal melanoma model correlate with aggressiveness of human melanoma metastases. *Molecular cancer research : MCR*, 6(5), 760–769. <https://doi.org/10.1158/1541-7786.MCR-07-0344>
36. Buenrostro, J. D., Wu, B., Chang, H. Y., & Greenleaf, W. J. (2015). ATAC-seq: A Method for Assaying Chromatin Accessibility Genome-Wide. *Current protocols in molecular biology*, 109, 21.29.1–21.29.9. <https://doi.org/10.1002/0471142727.mb2129s109>
37. Terranova, C., Tang, M., Orouji, E., Maitituoheti, M., Raman, A., Amin, S., Liu, Z., & Rai, K. (2018). An Integrated Platform for Genome-wide Mapping of Chromatin States Using High-throughput ChIP-sequencing in Tumor Tissues. *Journal of visualized experiments : JoVE*, (134), 56972. <https://doi.org/10.3791/56972>

38. Buenrostro, J. D., Giresi, P. G., Zaba, L. C., Chang, H. Y., & Greenleaf, W. J. (2013). Transposition of native chromatin for fast and sensitive epigenomic profiling of open chromatin, DNA-binding proteins and nucleosome position. *Nature methods*, 10(12), 1213–1218.
<https://doi.org/10.1038/nmeth.2688>.
39. Zhou, B., Wang, L., Zhang, S., Bennett, B. D., He, F., Zhang, Y., Xiong, C., Han, L., Diao, L., Li, P., Fargo, D. C., Cox, A. D., & Hu, G. (2016). INO80 governs superenhancer-mediated oncogenic transcription and tumor growth in melanoma. *Genes & development*, 30(12), 1440–1453.
<https://doi.org/10.1101/gad.277178.115>
40. Robertson, G., Hirst, M., Bainbridge, M., Bilenky, M., Zhao, Y., Zeng, T., Euskirchen, G., Bernier, B., Varhol, R., Delaney, A., Thiessen, N., Griffith, O. L., He, A., Marra, M., Snyder, M., & Jones, S. (2007). Genome-wide profiles of STAT1 DNA association using chromatin immunoprecipitation and massively parallel sequencing. *Nature methods*, 4(8), 651–657.
<https://doi.org/10.1038/nmeth1068>
41. Heintzman, N. D., Hon, G. C., Hawkins, R. D., Kheradpour, P., Stark, A., Harp, L. F., Ye, Z., Lee, L. K., Stuart, R. K., Ching, C. W., Ching, K. A., Antosiewicz-Bourget, J. E., Liu, H., Zhang, X., Green, R. D., Lobanenkov, V. V., Stewart, R., Thomson, J. A., Crawford, G. E., Kellis, M., ... Ren, B. (2009). Histone modifications at human enhancers reflect global cell-type-specific gene expression. *Nature*, 459(7243), 108–112.
<https://doi.org/10.1038/nature07829>

42. Orlova, N. N., Bogatova, O. V., & Orlov, A. V. (2020). High-performance method for identification of super enhancers from ChIP-Seq data with configurable cloud virtual machines. *MethodsX*, 7, 101165.
<https://doi.org/10.1016/j.mex.2020.101165>
43. Kuzume, A., Chi, S., Yamauchi, N., & Minami, Y. (2020). Immune-Checkpoint Blockade Therapy in Lymphoma. *International journal of molecular sciences*, 21(15), 5456. <https://doi.org/10.3390/ijms21155456>
44. Chen, L., & Han, X. (2015). Anti-PD-1/PD-L1 therapy of human cancer: past, present, and future. *The Journal of clinical investigation*, 125(9), 3384–3391.
<https://doi.org/10.1172/JCI80011>
45. Patel, S. A., & Minn, A. J. (2018). Combination Cancer Therapy with Immune Checkpoint Blockade: Mechanisms and Strategies. *Immunity*, 48(3), 417–433. <https://doi.org/10.1016/j.immuni.2018.03.007>
46. Conway, J. R., Kofman, E., Mo, S. S., Elmarakeby, H., & Van Allen, E. (2018). Genomics of response to immune checkpoint therapies for cancer: implications for precision medicine. *Genome medicine*, 10(1), 93.
<https://doi.org/10.1186/s13073-018-0605-7>
47. Morrison A. J. (2017). Genome maintenance functions of the INO80 chromatin remodeller. *Philosophical transactions of the Royal Society of London. Series B, Biological sciences*, 372(1731), 20160289.
<https://doi.org/10.1098/rstb.2016.0289>
48. Scott, K. L., Nogueira, C., Heffernan, T. P., van Doorn, R., Dhakal, S., Hanna, J. A., Min, C., Jaskelioff, M., Xiao, Y., Wu, C. J., Cameron, L. A., Perry, S. R.,

- Zeid, R., Feinberg, T., Kim, M., Vande Woude, G., Granter, S. R., Bosenberg, M., Chu, G. C., DePinho, R. A., ... Chin, L. (2011). Proinvasion metastasis drivers in early-stage melanoma are oncogenes. *Cancer cell*, 20(1), 92–103.
<https://doi.org/10.1016/j.ccr.2011.05.025>
49. Zhou, B., Wang, L., Zhang, S., Bennett, B. D., He, F., Zhang, Y., Xiong, C., Han, L., Diao, L., Li, P., Fargo, D. C., Cox, A. D., & Hu, G. (2016). INO80 governs superenhancer-mediated oncogenic transcription and tumor growth in melanoma. *Genes & development*, 30(12), 1440–1453.
<https://doi.org/10.1101/gad.277178.115>
50. Platanias L. C. (2005). Mechanisms of type-I- and type-II-interferon-mediated signalling. *Nature reviews. Immunology*, 5(5), 375–386.
<https://doi.org/10.1038/nri1604>
51. Dupont S. (2016). Role of YAP/TAZ in cell-matrix adhesion-mediated signalling and mechanotransduction. *Experimental cell research*, 343(1), 42–53. <https://doi.org/10.1016/j.yexcr.2015.10.034>
52. Qiao, Y., Chen, J., Lim, Y. B., Finch-Edmondson, M. L., Seshachalam, V. P., Qin, L., Jiang, T., Low, B. C., Singh, H., Lim, C. T., & Sudol, M. (2017). YAP Regulates Actin Dynamics through ARHGAP29 and Promotes Metastasis. *Cell reports*, 19(8), 1495–1502.
<https://doi.org/10.1016/j.celrep.2017.04.075>
53. Eschweiler, S., Clarke, J., Ramírez-Suástegui, C., Panwar, B., Madrigal, A., Chee, S. J., Karydis, I., Woo, E., Alzetani, A., Elsheikh, S., Hanley, C. J., Thomas, G. J., Friedmann, P. S., Sanchez-Elsner, T., Ay, F., Ottensmeier, C.

- H., & Vijayanand, P. (2021). Intratumoral follicular regulatory T cells curtail anti-PD-1 treatment efficacy. *Nature immunology*, 10.1038/s41590-021-00958-6. Advance online publication. <https://doi.org/10.1038/s41590-021-00958-6>
54. Sato, H., Niimi, A., Yasuhara, T., Permata, T., Hagiwara, Y., Isono, M., Nuryadi, E., Sekine, R., Oike, T., Kakoti, S., Yoshimoto, Y., Held, K. D., Suzuki, Y., Kono, K., Miyagawa, K., Nakano, T., & Shibata, A. (2017). DNA double-strand break repair pathway regulates PD-L1 expression in cancer cells. *Nature communications*, 8(1), 1751. <https://doi.org/10.1038/s41467-017-01883-9>

Vita

Seenya Vincent was born in Kerala, India, the daughter of Vincent Mahapillai and Alice Vincent. After spending much of her childhood in South Africa, Seenya moved with her parents and younger brother to the United States and settled in Houston, Texas. She graduated from Sharpstown High School, Houston, Texas before earning her Bachelor of Science in Chemistry from the University of Houston-Downtown. For the next few years, Seenya worked as a Research Assistant at UTHealth. In August of 2018, she entered The University of Texas MD Anderson Cancer Center UTHealth Graduate School of Biomedical Sciences.

Permanent address:

8523 Hazen St.

Houston, TX 77036